

Collective fluid dynamics of a polariton condensate in a semiconductor microcavity

A. Amo¹, D. Sanvitto¹, F. P. Laussy², D. Ballarini¹, E. del Valle², M. D. Martin¹, A. Lemaître³, J. Bloch³, D. N. Krizhanovskii⁴, M. S. Skolnick⁴, C. Tejedor² & L. Viña¹

Semiconductor microcavities offer unique systems in which to investigate the physics of weakly interacting bosons. Their elementary excitations, polaritons—mixtures of excitons and photons—can accumulate in macroscopically degenerate states to form various types of condensate in a wide range of experimental configurations, under either incoherent^{1,2} or coherent^{3,4} excitation. Condensates of polaritons have been put forward as candidates for superfluidity^{5,6}, and the formation of vortices⁷ as well as elementary excitations with linear dispersion⁸ are actively sought as evidence to support this. Here, using a coherent excitation triggered by a short optical pulse, we have created and set in motion a macroscopically degenerate state of polaritons that can be made to collide with a variety of defects present in the microcavity. Our experiments show striking manifestations of a coherent light–matter packet, travelling at high speed (of the order of one per cent of the speed of light) and displaying collective dynamics consistent with superfluidity, although one of a highly unusual character as it involves an out-of-equilibrium dissipative system. Our main results are the observation of a linear polariton dispersion accompanied by diffusionless motion; flow without resistance when crossing an obstacle; suppression of Rayleigh scattering; and splitting into two fluids when the size of the obstacle is comparable to the size of the wave packet. This work opens the way to the investigation of new phenomenology of out-of-equilibrium condensates.

Below a critical temperature, bosons of a sufficiently high number density undergo Bose–Einstein condensation (BEC). Under this condition, the particles collapse into a macroscopic condensate with a common phase, showing collective quantum behaviour like superfluidity, quantised vortices, interference, and so on. Until recently, BEC was only observed in dilute atomic gases at microkelvin temperatures. Following the recent observations of non-equilibrium BEC in semiconductor microcavities at temperatures of ~ 10 K, using momentum-¹ and real-space² trapping, the goal is now to observe new quantum phenomena associated with condensates of polaritons. For the same reasons that these particles benefit from having features especially favourable for condensation, such as very high critical temperatures, it is expected that their superfluid properties would similarly be manifest with altogether different magnitudes, such as very high critical velocities. Because in their Bose-condensed phase they have shown many deviations from the cold-atom systems, it is a priori not clear to what extent their properties would coincide with or depart from those observed in atoms, among which quantized vortices⁹, frictionless motion¹⁰, linear dispersion of the elementary excitations¹¹ or, more recently, Čerenkov emission of a condensate flowing at supersonic velocities¹² are the clearest signatures of quantum fluid propagation.

Microcavity polaritons are two-dimensional bosons, of mixed electronic and photonic nature, formed by the strong coupling of excitons—confined in semiconductor quantum wells—with photons trapped in a micrometre-scale resonant cavity¹³. Owing to their photon fractions, polaritons can easily be excited by an external laser source and detected by light emission. However, unlike photons, they experience strong interparticle interactions, owing to their partially electronic fractions. The deep polariton dispersion causes the effective masses of these particles to be 10^4 – 10^5 times smaller than the free electron mass, resulting in a very low density of states. This allows for a high state occupancy even at relatively low excitation intensities. However, polaritons can exist for only a few picoseconds in the cavity before decaying into photons and thermal equilibrium is therefore never achieved. In this respect, a macroscopically degenerate state of polaritons departs strongly from an atomic Bose-condensed phase, especially in our experiment, where the condensate is formed from a coherent excitation. The experimental observations of spectral and momentum narrowing, spatial coherence and long-range order—which have been used as evidence for polariton BEC—have also been seen in a pure photonic laser¹⁴. The recent observation of long-range spatial coherence¹⁵, vortices⁷ and the loss of coherence with increasing density in the condensed phase^{16,17} are in accordance with macroscopic phenomena observed in interacting, coherent bosons. However, a study of the fluid dynamics of coherent states of this kind is still missing.

In this work, using a combination of temporally and spatially resolved spectroscopic techniques in a GaAs microcavity¹⁸, we are able to probe directly the dynamics of the motion of a condensed droplet of polaritons by tracking its space-time evolution. We report a shape-preserving, non-diffusive propagation of matter, dressed by the light field, moving at a speed of the order of 10^6 m s⁻¹. Collisions with obstacles of different sizes provide further insights into the dynamics of this system: the collective behaviour shown here is expected from a condensate of polaritons, as suggested by our theoretical analysis in terms of a nonlinear Schrödinger equation. Our findings are a class of new phenomena that, like some previously observed^{17,8}, are consistent with superfluidity and nonlinear optical effects¹⁹. However, our work, which probes the dynamics of a condensate, adds insight into the extent to which the polariton condensate exhibits superfluid-like properties.

Our experiments are based on the continuous replenishment of a polariton fluid, at energy E_s and momentum $\hbar\mathbf{k}_s$, from a higher-lying state, at E_p and $\hbar\mathbf{k}_p$, driven coherently by a continuous-wave laser and set in motion by a short trigger pulse (2 ps) at the idler state, E_1 and $\hbar\mathbf{k}_1$, in a configuration of a triggered optical parametric oscillator (TOPO; see Fig. 1 and Supplementary Information)²⁰. This experimental arrangement allows the study of the propagation of the signal

¹Departamento Física de Materiales, ²Departamento Física Teórica de la Materia Condensada, Universidad Autónoma de Madrid, 28049 Madrid, Spain. ³LPN/CNRS, Route de Nozay, 91460 Marcoussis, France. ⁴Department of Physics & Astronomy, University of Sheffield, Sheffield S3 7RH, UK.

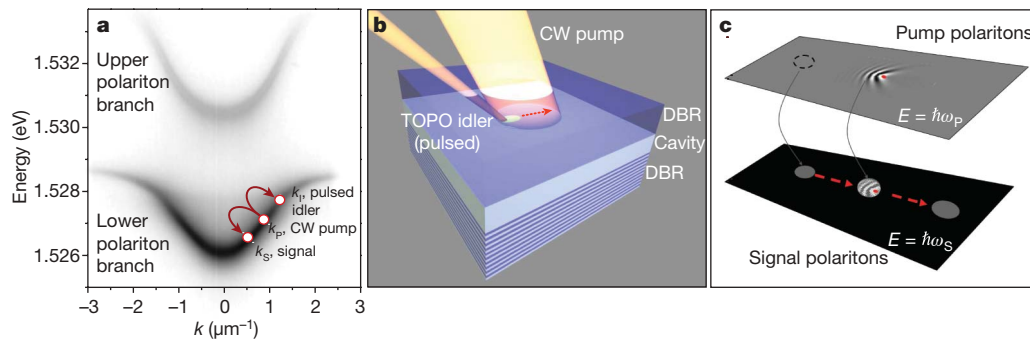


Figure 1 | Experimental configuration of the TOPO. **a**, Experimental microcavity dispersion of the two polariton branches, showing the condition of excitation of the continuous pump and the formation of a polariton state at the continuous-wave (CW) pump energy, which feeds the signal polaritons at a lower energy, fulfilling the conditions $2k_p = k_s + k_i$ and $2E_p = E_s + E_i$. This process is initialised by a pulse at the idler state. **b**, Diagram of the experimental set-up. The two laser beams are shown impinging on the sample surface at an arbitrary direction (x) in the plane of the cavity (x, y). The polaritons are created in the cavity region (light green

polaritons, which can have any, specifically selected, in-plane momentum $\hbar\mathbf{k}$ given by the phase matching conditions shown in the caption of Fig. 1. Owing to the polariton light emission, we are able to probe continuously and in real time features such as the motion of the droplet and its dispersion.

The experimental dispersions of the light emitted by the polaritons in different regimes are depicted in Fig. 2a. The false-colour graph in the upper panel shows the emission of the polariton fluid generated by the TOPO, after the trigger pulse has disappeared; in the lower panel this is compared with the standard parabolic dispersion of the photoluminescence obtained under non-resonant, low-power excitation. The most striking feature, under TOPO conditions, is the clear linearization of the dispersion around the signal state. This dispersion arises from the nonlinear response as a manifestation of dominant interactions that strongly dress the states, and resembles the Bogoliubov dispersion for elementary excitations of a superfluid. In the latter case, linearization leads to suppression of weak scattering and therefore to motion without dissipation. In our case, the dispersion reflects the

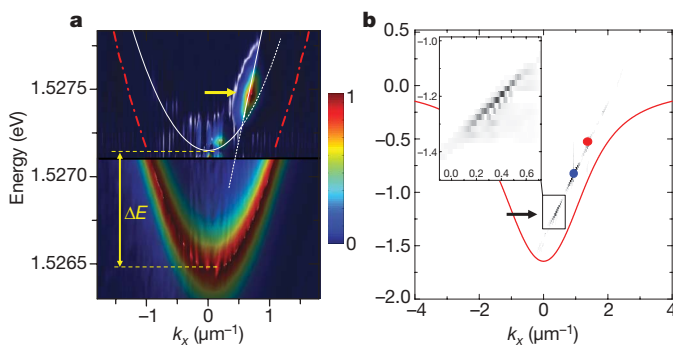


Figure 2 | Experimental and theoretical dispersions. **a**, Upper panel: false-colour plot of the polariton dispersion under TOPO conditions, showing intensity of emitted light (arbitrary units); lower panel: dispersion obtained under non-resonant, low-power excitation, for which polaritons are not in a condensed state. It is important to notice that the dispersion in which the signal polaritons are moving (bright spot denoted by the arrow in the upper panel) is different from the bare dispersion and shows a linear dependence on k_x . The energy blueshift, $\Delta E = 0.6$ meV, is due to polariton–polariton interactions. **b**, Computer simulation of $|\psi(k_x, E)|^2$ showing the linearization of the signal polariton dispersion due to stimulated scattering processes occurring between a CW pump (blue circle) and a probe (red circle) after the pulse has disappeared. The vertical axis shows the bare exciton energy. An expanded plot of the region around the signal is depicted in the inset. The red line describes the bare dispersion relation of polaritons.

circle), which is surrounded by two highly reflective distributed Bragg reflectors (DBRs). **c**, Sketch of the motion of two fluids, pump polaritons (upper) and signal polaritons (lower), against a defect depicted by the red point. Although the two fluids are spatially in the same plane, they are shown separately in the figure to emphasize their energy difference. The movement of the signal polariton fluid, at $E_s = \hbar\omega_s$, is represented by the circle moving from left to right on the black plane. The continuous feeding from the pump polaritons at $E_p = \hbar\omega_p$, shown in the grey plane, makes it possible to detect this motion. \hbar , Planck's constant (\hbar) divided by 2π .

dynamics of the whole system, rather than that of its excitations only. Figure 2a also shows that, for the TOPO, polaritons are blueshifted ($\Delta E = 0.6$ meV at $k \equiv |\mathbf{k}| = 0$), owing to polariton–polariton interactions, and that the intensity peaks strongly at $k_s = 0.6 \mu\text{m}^{-1}$, which is determined by the phase-matching conditions ($2k_p = k_s + k_i$).

Our system involves macroscopically degenerate states of bosons coupled through exciton–exciton interactions. It can therefore be described theoretically using a nonlinear Schrödinger equation for the polariton wavefunction, $\psi(x, t)$, in the presence of a continuous pump, F_p , and a pulse, F_i , that are incident on the microcavity with respective momenta $\hbar\mathbf{k}_p$ and $\hbar\mathbf{k}_i$, have frequencies ω_p and ω_i , and are localized in Gaussian spots located at x_p and x_i , with spatial extensions σ_p and σ_i . The pulse hits the microcavity at time t_i with a Gaussian profile of root-mean-square duration σ_t . The Schrödinger equation is thus

$$i\hbar \frac{\partial \psi(x, t)}{\partial t} = \left(D - i\hbar \frac{\gamma}{2} + V |\psi(x, t)|^2 \right) \psi(x, t) + F_p e^{-(x-x_p)^2/2\sigma_p^2} e^{i(k_p x - \omega_p t)} + F_i e^{-(x-x_i)^2/2\sigma_i^2} e^{-(t-t_i)^2/2\sigma_t^2} e^{i(k_i x - \omega_i t)} \quad (1)$$

where the operator D is the free-propagation energy of the particles; in our case, it provides the dispersion relation specific to polariton branches. The lower branch gives rise to the OPO ($F_i = 0$) or TOPO ($F_i \neq 0$) physics of phase-matched scattering. The two last terms are responsible for maintaining the system out of equilibrium against the decay rate γ . The inclusion of these terms is a crucial difference between our case and the usual case of atomic condensates. Figure 2b shows the calculated dispersion in TOPO conditions, which reproduces both the linearization induced by the interactions and a strong signal-idler emission that proves the triggering of OPO scattering.

In Fig. 3, real-space images of the signal polaritons are shown along with their counterparts in momentum space. The images show that the polariton droplet undergoes unperturbed motion without diffusion in either the x or the y direction, proving that the dispersion around the signal state has lost its locally parabolic character. At the same time, the packet also conserves a well-defined momentum during the propagation time (Fig 3b). This confirms that the polariton signal has a linearized dispersion, as predicted theoretically and observed experimentally (see Fig. 2). By contrast, at low pump powers (without linearization of the dispersion), we observe the very fast appearance of the Rayleigh scattering circle in reciprocal space⁶ and the absence of collective motion in real space (Supplementary

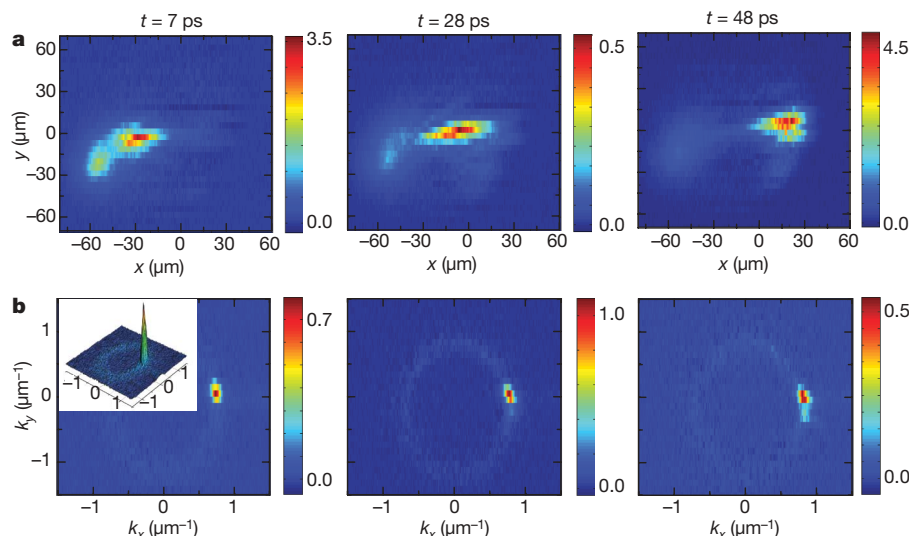


Figure 3 | Free movement of a polariton droplet. **a**, Spectrally selected observation at the TOPO signal energy of a coherent polariton gas moving at group velocity $v_g = 1.2 \times 10^6 \text{ m s}^{-1}$ from left to right without being perturbed. Colour scale is as in Fig. 2. The images, recorded under similar conditions to those of Fig. 2, are real-space shots taken at different times

(shown) after the pulse arrival ($t = 0$). The total polariton density (pump, signal and idler) is estimated to be of the order of $10^2 \mu\text{m}^{-2}$. **b**, Same conditions as in **a** but in momentum space. The inset displays a three-dimensional view which shows the narrow k distribution. Supplementary Videos 3 and 4 show the free polariton motion.

Videos 1, 2). This observation demonstrates the suppression of scattering as we cross the threshold into the coherent regime.

This propagation is reproduced by our numerical simulation, as seen in Fig. 4a, where a snapshot of the signal is shown at regular intervals of times. To observe the motion of the signal, we take advantage of its separation in energy from both the idler and the pump by filtering the emission in a window of energy, as done in the experiments. Clear propagation within the excitation spot is sustained from the time the pulse triggers the OPO (~ 2 ps), until the time the signal reaches the edge of the excitation spot. It has a constant speed of $(0.95 \pm 0.1) \times 10^6 \text{ m s}^{-1}$, in agreement with that obtained experimentally ($(1.2 \pm 0.3) \times 10^6 \text{ m s}^{-1}$). In Fig. 4b, the spread of the polariton wave packet is plotted as a function of time both from the experimental data and according to calculations based on a parabolic or linear dispersion. The calculation shows that, without the linearization due to interactions, the wave packet would expand more than twice as much during the same time of flight. Moreover, the agreement with the experiments using equation (1) implies that polariton interactions are responsible for the linearization of the signal state.

The excitations of the polariton fluids created with a TOPO can be studied by observing their collisions with structural defects, which are naturally present in the sample. Figure 5a shows images obtained in the near field of a polariton fluid colliding with a defect occurring in the middle of its trajectory. In the course of its propagation, the signal shows unambiguous signs of passing through a defect. However, it clearly maintains its cohesion in this process. This is most strikingly observed in momentum space (Fig. 5b), where the signal is left completely unaltered until the very end of the trajectory, when the single-state occupancy starts spreading as the signal dies by moving off the edge of the pump laser region.

We note that the images reflect the addition of two different contributions: that of the pump polaritons (extended in an area of $\sim 8 \times 10^3 \mu\text{m}^2$) and that of the signal polaritons themselves, which, being constantly fed by the pump, reflect its density fluctuations. Figure 1c illustrates how these two contributions are detected at the signal polariton energy. The fringes observed around the defect appear as a result of the local change in density of the pump polaritons, which is reflected in the spatial structure of the signal.

The pump polaritons are injected in a coherent state, at high energy, density and momenta and with a group velocity greater than the speed of sound, $v_s = 3 \times 10^6 \text{ m s}^{-1}$ (estimated from the blueshift

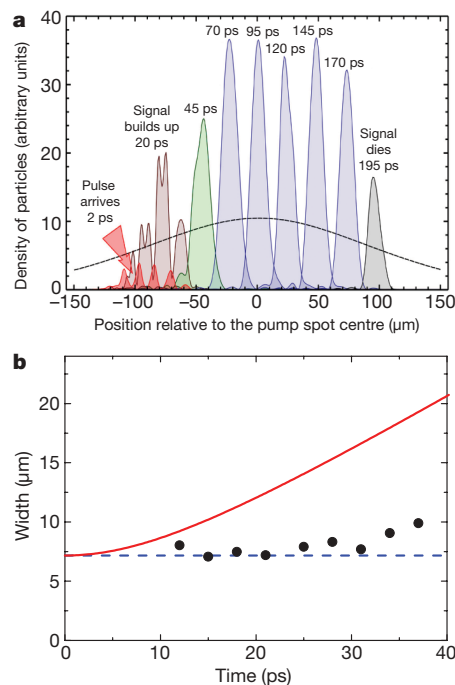


Figure 4 | Simulation of the travelling signal polariton state within the pump spot. **a**, Computer simulation showing the spatial extent of the pump polaritons (black dashed line) and the evolution of the signal wave packet. The signal is created (red) after a pulse has excited the microcavity at $k_1 = 2k_p - k_s$, builds up (orange) and develops into a well-defined Gaussian-like wave packet (green) that subsequently travels over hundreds of micrometres (blue) while inside the pump polariton area. The wave packet dies as it reaches the edge of the pump spot (grey). The animation of the simulated polariton dynamics in real and momentum space can be seen in the Supplementary Video 5. **b**, The measured width (black points) of the coherent polariton droplet as it flows unperturbed, plotted as a function of time. The blue dashed line shows the evolution expected for a fluid with a linear dispersion. The red solid line depicts the size of a polariton wave packet as obtained from the Schrödinger equation with a quadratic dispersion (diffusive regime).

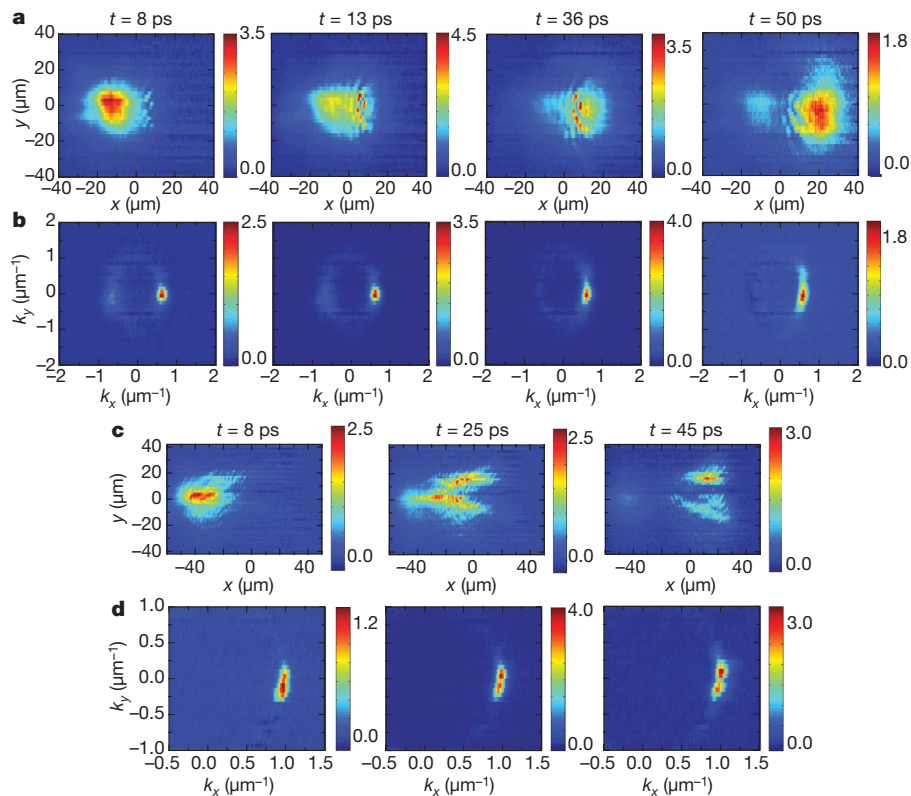


Figure 5 | Images of a polariton droplet colliding against native defects. **a, b**, A small structural defect in the sample is encountered in the trajectory of the polariton condensate moving at a velocity of $0.9 \times 10^6 \text{ m s}^{-1}$. Colour scale is as in Fig. 2. The position of the obstacle is revealed, in real space (**a**), by Čerenkov waves caused by the pump polaritons, which are travelling at a supersonic speed. However, the signal polaritons pass through the defect in a superfluid fashion without changing direction or scattering against the obstacle (clearer evidence of this phenomenon can be observed in

of the polariton dispersion), giving rise, in the presence of a defect, to characteristic quantum interferences resembling Čerenkov waves, which are observed through the emission of the signal polaritons. Similar shock waves have been reported recently for an atomic BEC flowing against a potential barrier at Mach numbers greater than one¹². It is important to note that the visibility of these waves does not imply that the signal polaritons are also in the ‘Čerenkov regime’. By contrast, for the signal polaritons (which are at lower energy and momentum), the group velocity ($0.9 \times 10^6 \text{ m s}^{-1}$) is less than v_s , and the signal polariton droplet can thus be expected to behave as a superfluid: excitations in the droplet are inhibited while it passes through the obstacle.

In Fig. 5c, d, a more striking collision is observed: one in which the size of the defect is comparable to that of the polariton packet. The finite-size travelling polariton fluid scatters coherently and elastically on the potential and is split in two after the collision. We note that the process is dissipationless. A normal polariton fluid^{21,22} would diffuse both in real and reciprocal space in this configuration. Our macroscopically degenerate droplet, the dispersion of which has been linearized, instead follows coherent and diffusionless trajectories, as borne out by our experiments and clearly shown in the real-space images of Fig. 5c, albeit with two new momenta (see Fig. 5d). The linear dispersion is the key element of this coherent propagation, as any scattered particle from the wave packet remains in phase with the others and at the same group velocity, precluding diffusion both in real and in reciprocal space. We again note that this concerns the wave packet itself, not only its excitations, as is the case in the Landau picture of helium superfluidity. The system exhibits the dynamics of a condensate, but many new features arise from the specific properties of polaritons. Until now, theoretical

Supplementary Video 6). This fact is confirmed by the images taken at the same times in momentum space (**b**). It is clear that the momentum vector does not change significantly when the condensate crosses the obstacle (Supplementary Video 7). **c, d**, The polariton fluid encounters a defect of a size comparable to its own: the condensed state fully experiences the defect potential, which strongly perturbs the trajectory in real space (**c**) showing the appearance of two independent polariton states with different momentum vectors (**d**); see also Supplementary Videos 8 and 9.

analysis of the scattering has only been made in the perturbative regime^{6,23}, with regard to the elementary excitations of the polariton condensate.

Our findings call for further work, both experimental and theoretical, to reveal other properties of this unusual state of matter: a coherent, macroscopically occupied Bose fluid propagating at ultra-high speed. We have demonstrated that semiconductor microcavities are ideal candidates to study exotic bosonic phenomena. Although the physics associated with condensed phases of polaritons presents both fundamental and subtle deviations from the atomic case, these may prove to be assets in their future study. For instance, in a dissipative system, particle number conservation is lifted and a well-defined phase can be externally imprinted onto polaritons, allowing the investigation of symmetry-breaking mechanisms.

METHODS SUMMARY

Time- and space-resolved emission is obtained at 5 K under simultaneous continuous-wave and pulsed laser excitation. The polariton fluid, at energy E_S and momentum k_S , is continuously replenished from a higher-lying state, at E_P and k_P , by the continuous-wave laser and set in motion by a short trigger pulse (2 ps) at the idler state, E_I and k_I , in a configuration of a TOPO (Fig. 1). Typically, the pump injects a coherent polariton state into the lower polariton branch at an angle of 10° relative to the normal to the cavity plane; the pulse arrives at time $t = 0$ in resonance with the branch at 16° , triggering the OPO and generating a polariton signal with a finite momentum at 4° . Images of the near and far fields of a GaAs-based microcavity are projected on to the entrance slit of a 0.5-m imaging spectrometer attached to a streak camera, thus allowing for simultaneous collection of two-dimensional, time-resolved images at a given energy. To avoid problems caused by detection at the pulsed laser energy, which would bleach the streak camera, the pulsed laser is made resonant with the idler rather than with

the signal state of the triggered OPO. Furthermore, to retain only the light emission from the TOPO signal, the OPO-only emission coming from the pump field, contributing at $k = 0$, is subtracted from all the images.

To solve the nonlinear Schrödinger equation, equation (1) is integrated numerically, first in the absence of the pulse ($F_1 = 0$), until a steady state is reached for $|\psi(x, t)|^2$. We obtain the energy/momentum-density plot of the system by Fourier-transforming $\psi(x, t)$. At a given time, t_i , we release a Gaussian pulse ($F_1 \neq 0$) that triggers OPO processes. We track the new evolution of $\psi(x, t)$ until the steady state is restored, and Fourier-transform again during this time. In order to compare with the experiment, we subtract the two dispersions.

Full Methods and any associated references are available in the online version of the paper at www.nature.com/nature.

Received 26 August; accepted 13 November 2008.

1. Kasprzak, J. *et al.* Bose–Einstein condensation of exciton polaritons. *Nature* **443**, 409–414 (2006).
2. Balili, R., Hartwell, V., Snoke, D., Pfeiffer, L. & West, K. Bose-Einstein condensation of microcavity polaritons in a trap. *Science* **316**, 1007–1010 (2007).
3. Stevenson, R. M. *et al.* Continuous wave observation of massive polariton redistribution by stimulated scattering in semiconductor microcavities. *Phys. Rev. Lett.* **85**, 3680–3683 (2000).
4. Saba, M. *et al.* High-temperature ultrafast polariton parametric amplification in semiconductor microcavities. *Nature* **414**, 731–735 (2001).
5. Kavokin, A., Malpuech, G. & Laussy, F. P. Polariton laser and polariton superfluidity in microcavities. *Phys. Lett. A* **306**, 187–199 (2003).
6. Carusotto, I. & Ciuti, C. Probing microcavity polariton superfluidity through resonant Rayleigh scattering. *Phys. Rev. Lett.* **93**, 166401 (2004).
7. Lagoudakis, K. G. *et al.* Quantised vortices in an exciton–polariton fluid. *Nature Phys.* **4**, 706–710 (2008).
8. Utsunomiya, S. *et al.* Observation of Bogoliubov excitations in exciton-polariton condensates. *Nature Phys.* **4**, 700–705 (2008).
9. Abo-Shaeer, J. R., Raman, C., Vogels, J. M. & Ketterle, W. Observation of vortex lattices in Bose-Einstein condensates. *Science* **292**, 476–479 (2001).
10. Onofrio, R. *et al.* Observation of superfluid flow in a Bose-Einstein condensed gas. *Phys. Rev. Lett.* **85**, 2228–2231 (2000).
11. Steinhauer, J., Ozeri, R., Katz, N. & Davidson, N. Excitation spectrum of a Bose-Einstein condensate. *Phys. Rev. Lett.* **88**, 120407 (2002).
12. Carusotto, I., Hu, S. X., Collins, L. A. & Smerzi, A. Bogoliubov-Cerenkov radiation in a Bose-Einstein condensate flowing against an obstacle. *Phys. Rev. Lett.* **97**, 260403 (2006).
13. Weisbuch, C., Nishioka, M., Ishikawa, A. & Arakawa, Y. Observation of the coupled exciton-photon mode splitting in a semiconductor quantum microcavity. *Phys. Rev. Lett.* **69**, 3314–3317 (1992).
14. Bajoni, D., Senellart, P., Lemaître, A. & Bloch, J. Photon lasing in GaAs microcavity: Similarities with a polariton condensate. *Phys. Rev. B* **76**, 201305(R) (2007).
15. Lai, C. W. *et al.* Coherent zero-state and π -state in an exciton–polariton condensate array. *Nature* **450**, 529–532 (2007).
16. Krizhanovskii, D. N. *et al.* Dominant effect of polariton-polariton interactions on the coherence of the microcavity optical parametric oscillator. *Phys. Rev. Lett.* **97**, 097402 (2006).
17. Porras, D. & Tejedor, C. Linewidth of a polariton laser: Theoretical analysis of self-interaction effects. *Phys. Rev. B* **67**, 161310 (2003).
18. Perrin, M., Senellart, P., Lemaître, A. & Bloch, J. Polariton relaxation in semiconductor microcavities: Efficiency of electron-polariton scattering. *Phys. Rev. B* **72**, 075340 (2005).
19. Bolda, E. L., Chiao, R. Y. & Zurek, H. Dissipative optical flow in a nonlinear Fabry-Pérot cavity. *Phys. Rev. Lett.* **86**, 416–419 (2001).
20. Ballarini, D. *et al.* Observation of long-lived polariton states in semiconductor microcavities across the parametric threshold. Preprint at (<http://arxiv.org/abs/arXiv:0807.3224>) (2008).
21. Freixanet, T., Sermage, B., Tiberj, A. & Panel, R. In-plane propagation of excitonic cavity polaritons. *Phys. Rev. B* **61**, 7233–7236 (2000).
22. Langbein, W. *et al.* Polarization beats in ballistic propagation of exciton-polaritons in microcavities. *Phys. Rev. B* **75**, 075323 (2007).
23. Szymanska, M. H., Keeling, J. & Littlewood, P. B. Nonequilibrium quantum condensation in an incoherently pumped dissipative system. *Phys. Rev. Lett.* **96**, 230602 (2006).

Supplementary Information is linked to the online version of the paper at www.nature.com/nature.

Acknowledgements We thank I. Carusotto, M. Wouters and N. Berloff for discussions and D. Steel for a critical reading of the manuscript. This work was partially supported by the Spanish Ministerio de Educación y Ciencia (MEC) (MAT2005-01388, NAN2004-09109-C04-04 & QOIT-CSD2006-00019), the Comunidad Autónoma de Madrid (S-0505/ESP-0200) and the IMDEA-Nanociencia. D.B. and E.d.V. acknowledge a scholarship (Formación de Profesorado Universitario) of the Spanish MEC. D.S. and M.D.M. thank the Ramón y Cajal Programme.

Author Information Reprints and permissions information is available at www.nature.com/reprints. Correspondence and requests for materials should be addressed to D.S. (daniele.sanvitto@uam.es).

METHODS

Sample. The studied microcavity is composed of an AlAs $\lambda/2$ cavity with top and bottom Bragg mirrors of 15 and, respectively, 25 Al_{0.1}Ga_{0.9}As/AlAs pairs, grown on a GaAs substrate. A 20-nm-thick GaAs quantum well is embedded at the antinode position of the cavity mode. When the sample is kept at a temperature of 10 K, the heavy-hole excitons of the quantum well are strongly coupled with the cavity mode, with a Rabi splitting of 4.4 meV. The wedge-shaped cavity allows for fine-tuning of the resonance between the quantum well exciton and the cavity mode by changing the position of the excitation spot on the sample.

Experiments. To make polaritons flow, we have to address three important issues: the very short polariton dwell time in the cavity ($<2\text{--}5$ ps), which hinders detection of their dynamics; creation of polaritons in a state with a well-defined momentum; and spatial inhomogeneities produced by sample strain and/or defects. The signal polaritons, fed by the pump in resonance with the lower polariton branch, last for more than 10^{-9} s after the trigger pulse of 2 ps, thus allowing for the detection of the polariton flow dynamics. This approach addresses the first issue listed above: although the lifetime of a single particle of the polariton droplet remains short (a few picoseconds), the packet itself lasts hundreds of picoseconds. To reduce the effect of spatial inhomogeneities, which are present in all semiconductor microcavities^{24,25}, we keep the pump power at an intensity high enough that most of the potential fluctuations are smoothed out²⁶. Scattering centres are nevertheless still present with an approximate density of 10^{-2} μm^{-2} , but, as shown in the main text, they can help to reveal the peculiar quantum nature of the polariton fluid.

TOPO. A TOPO is an optical parametric amplifier (for an experimental description of a polariton OPA obtained under CW conditions, see ref. 27) in which the continuous-wave seed provided by an external probe at the idler state is substituted by a short pulse (2 ps), which simply initializes the system, inducing a population at the signal state. After the pulse has disappeared, the signal state is left macroscopically occupied, and the final-state stimulation of the pump polaritons to the signal polaritons carries on for hundreds of picoseconds even if the pulse is no longer present (see Supplementary Fig. 1). Our experimental TOPO configuration differs from the conventional realization of atomic Bose–Einstein condensates and superfluids formed spontaneously in thermal equilibrium without the action of any external driving field. In our case, owing to the lossy character of polaritons, an external coherent source must drive the system. Furthermore, the fluid has a finite spatial extension and propagates as a whole; hence, we are investigating the explicit kinematics of a droplet of BEC, rather than the indirect propagation of a defect inside an infinite-size system.

The propagation of a signal whose shape remains unaltered over great distances is suggestive of a soliton surfing on the steady-state OPO; this picture correctly includes the notion of a non-perturbative excitation (triggered by the pulse). However, elements that are crucial for the stability of a soliton, such as attractive rather than repulsive interactions or the dependence on the dimensionality of the system or on the particle densities, are not present in our case, and a plethora of different shapes, widths and heights of the wave packets can also be sustained on the same dispersion. Therefore, interactions serve the main purpose of replenishing the signal rather than holding it together, and the soliton description is thus not adequate. Instead, this system provides a coherent and macroscopic population of bosons isolated in energy on a linear dispersion. Both ingredients are essential in accounting for the experimental findings.

24. Gurioli, M. *et al.* Weak localization of light in a disordered microcavity. *Phys. Rev. Lett.* **94**, 183901 (2005).
25. Sanvitto, D. *et al.* Spatial structure and stability of the macroscopically occupied polariton state in the microcavity optical parametric oscillator. *Phys. Rev. B* **73**, 241308(R) (2006).
26. Malpuech, G., Solnyshkov, D. D., Ouerdane, H., Glazov, M. M. & Shelykh, I. Bose glass and superfluid phase of cavity polaritons. *Phys. Rev. Lett.* **98**, 206402 (2007).
27. Sanvitto, D., Whittaker, D. M., Skolnick, M. S. & Roberts, J. S. Continuous wave pump-probe experiment on a planar microcavity. *Phys. Stat. Sol. (a)* **202**, 353–356 (2005).